

# Compact Objects by Extended Gravitational Decoupling in $f(G, T)$ Gravity

M. Sharif<sup>1</sup> \*and K. Hassan<sup>2</sup> †

<sup>1</sup> Department of Mathematics and Statistics, The University of Lahore,  
1-KM Defence Road Lahore, Pakistan.

<sup>2</sup> Department of Mathematics, University of the Punjab,  
Quaid-e-Azam Campus, Lahore-54590, Pakistan.

## Abstract

In this paper, we investigate the anisotropic interior spherically symmetric solutions by utilizing the extended gravitational decoupling method in the background of  $f(G, T)$  gravity, where  $G$  and  $T$  signify the Gauss-Bonnet term and trace of the stress-energy tensor, respectively. The anisotropy in the interior geometry arises with the inclusion of an additional source in the isotropic configuration. In this technique, the temporal and radial potentials are decoupled which split the field equations into two independent sets. Both sets individually represent the isotropic and anisotropic configurations, respectively. The solution corresponding to the first set is determined by using the Krori-Barua metric potentials whereas the second set contains unknown which are solved with the help of some constraints. The ultimate anisotropic results are evaluated by combining the solutions of both distributions. The influence of decoupling parameter is examined on the matter variables as well as anisotropic factor. We illustrate the viable and stable features of the constructed solutions by using energy constraints and three stability criteria, respectively.

---

\*msharif.math@pu.edu.pk

†komalhassan3@gmail.com

Finally, we conclude that the obtained solutions are viable as well as stable for the whole domain of the coupling parameter.

**Keywords:** Self-gravitating systems; Stability; Gravitational decoupling;  $f(G, T)$  gravity.

**PACS:** 04.20.Jb; 04.50.Kd; 04.40.Dg.

## 1 Introduction

The gigantic cosmos contains systematic structures ranging from small bodies to massive configurations like clouds, stars, clusters, super-clusters and galaxies. A widely recognized theory, general relativity (GR), has played an essential role in comprehending the mysterious features and evolution of the universe. It is assumed that our cosmos is comprised of ordinary source, dark matter and dark energy. The visible part of the universe is ordinary matter, while dark matter and dark energy have some ambiguous and enigmatic nature, which are supposed to be well delineated by GR. Further, it helps in resolving the velocity curves of galaxies [1] together with accelerated cosmic expansion [2]. The presence of dark energy was explicated by accommodating the cosmological constant into the Lambda cold dark matter ansatz. Nevertheless, the readjustment of the values of cosmological constant is highly needed in order to describe the dynamics of the universe through several cosmic eras and its matching with the observational data. Thus, to resolve these issues, modified gravity theories are regarded as the favorable alternatives to GR. The Einstein-Hilbert action is altered to obtain the modified theories by either adding or replacing the scalar curvatures and their related generic functions.

The forthright generalization of GR in higher dimensions is the Lovelock theory of gravity, which becomes equivalent to GR in 4-dimensions [3]. This theory yields two scalars, the first one is the Ricci scalar  $R$  (also called as the first Lovelock scalar), and the second one is the Guass-Bonnet invariant (GB) (dubbed as the second Lovelock scalar). Another way of modifying action is achieved with the help of second lovelock scalar (GB invariant) which gives rise to Einstein GB gravity in 5-dimensions [4]. The GB term in mathematical notation is denoted as

$$G = R^{\sigma\nu\mu} R_{\sigma\nu\mu} - 4R^{\sigma} R_{\sigma} + R^2,$$

which is presented as a conjunction of the curvature scalar, Ricci tensor ( $R_{\zeta\sigma}$ ) and curvature tensor ( $R_{\zeta\sigma\nu\mu}$ ). It is a 4-dimensional invariant and free from spin-2 ghost instabilities. To understand the effects of GB invariant in four dimensions, Nojiri and Odintsov [5] modified the Einstein-Hilbert action by including the generic function  $f(G)$  which led to  $f(G)$  gravity or modified GB theory. This gravity is supposed to investigate the progression from decelerated to accelerated phase as well as adequately describes the salient aspects of cosmic expansion.

One of the simplest extension of GR is introduced by substituting  $R$  with its generic  $f(R)$  function in the Lagrangian, namely  $f(R)$  gravity. Several researchers utilized the feasible  $f(R)$  models to examine the inflationary and cosmic acceleration of the universe [6]. Bertolami et al [7] first proposed the concept of matter-geometry coupling in  $f(R)$  theory, using Lagrangian as a function of  $R$  and  $\mathcal{L}_m$  to investigate the effects of this interaction on massive objects. This interaction prompted many researchers to focus their attention on proposing a coupling that helps in studying the fast cosmic expansion efficiently. In this respect, Harko et al [8] coupled matter and geometric expressions in the Einstein-Hilbert action and introduced  $f(R, T)$  theory.

Sharif and Ikram [9] proposed another non-minimal coupled gravity, i.e.,  $f(G, T)$  theory and discussed energy conditions in FRW universe. In this theory, the energy-momentum tensor (EMT) is not conserved and test particles follow the non-geodesic track as a result of an extra force. The addition of  $T$  along with  $G$  significantly demonstrates the fascinating outcomes regarding the present cosmos. The same authors [10] studied the stability of some cosmological models via linear perturbation in the realm of isotropic and homogeneous cosmos. Mustafa et al. [11] examined the necessary physical properties of three compact objects possessing anisotropic configurations and obtained well-behaved solutions in  $f(G, T)$  gravity. We have decomposed the Riemann tensor using Herrera approach to evaluate the complexity factor in the static cylindrical structure (uncharged-charged), which was further discussed for non-static uncharged and charged spherical as well as cylindrical geometries [12].

In dense compact entities, the interactions of substances exhibit distinct characteristics in different directions that ensure the existence of anisotropy within the compact structures [13]. Anisotropy in the inner configurations is believed to be induced by phase transition [14] and superfluid [15]. Herrera and Santos [16] looked at the causes of anisotropy as well as how it affected the progression of astrophysical objects. By using a specific anisotropic fac-

tor, Harko and Mak [17] were able to study the anisotropic static spherical structures through the analytical solution of the field equations. Dev and Gleiser [18] determined exact solutions of the field equations using different forms of the equation of state relating tangential as well as radial pressure and examined the remarkable influence of pressure anisotropy on physical attributes of celestial objects. Paul and Deb [19] studied the anisotropic stellar entities in hydrostatic equilibrium. Arbanil and Malheiro [20] investigated the stability of anisotropic strange stars through numerical solutions by employing MIT bag model.

There exist a number of past related works on the solutions of the gravitational field equations in different modified theories which can be used to model physically acceptable compact bodies. In GR, Errehymy et al [21] studied the substantial features of anisotropic celestial bodies which were found to be less dense. Moreover, it can be observed that along with the less dense stellar stars in GR, only the radial component of adiabatic index is utilized in evaluating their realistic configurations [22]. The graphical analysis of compact stars in  $f(G)$  gravity is assessed without utilizing the adiabatic index criterion by several researchers [23]. A similar pattern is followed by Shamir and Zia [24] in the framework of  $f(R, G)$  gravity.

The vague nature of astrophysical systems is obtained through analytic solutions of the field equations. The field equations contain several geometric ingredients and are highly nonlinear, making it challenging to compute such solutions. Due to the non-linear behavior, researchers have always been interested to develop specific procedure that can be utilized to solve these equations and provide physically feasible results. In order to address this issue, a recently developed technique so called gravitational decoupling via minimal geometric deformation (MGD) has proven helpful in determining the feasible anisotropic solutions. Primarily, Ovalle [25] implemented this technique to find new anisotropic spherical solutions. Afterwards, Ovalle et al. [26] calculated the anisotropic domains by generalizing the isotropic system and analyzed them graphically. Gabbanelli et al. [27] worked on Durgapal-Fuloria solution to compute the anisotropic solution.

Estrada and Tello-Ortiz [28] employed the gravitational decoupling to formulate new analytic anisotropic stellar models and graphically analyze their physical features. Singh et al. [29] investigated interior anisotropic solutions in class-I spacetime and estimated the radius along with mass of compact bodies through  $M-R$  curve. Hensh and Stuchlik [30] utilized the Tolman VII solution as a seed source for computing its anisotropic version.

Sharif and Saba [31] used the known solution for the perfect source and explored the physical properties of the charged-uncharged anisotropic domains in  $f(G)$  gravity. A substantial body of research has been done to produce the anisotropic interior solutions using this technique in different modified theories [32]. Recently, we have discussed new anisotropic models corresponding to Tolman V, Krori-Barua ansatz and Karmarkar condition for uncharged and charged spherical geometries through MGD. Further, the extended geometric deformation method has also been applied to analyze the constructed anisotropic solutions in  $f(G, T)$  theory [33].

In MGD technique, only the radial coefficient is distorted while keeping the temporal part unperturbed, hence leads to some limitations. In this approach, there is no energy transmission between matter sources, so the only interaction is gravitational. Ovalle [34] proposed an extension of MGD which also decouples the temporal coordinate along with the radial, termed as extended gravitational decoupling (EGD). Contreras and Bargueno [35] applied this approach for 2+1 dimensional spacetime to extend the charged BTZ solution by addressing vacuum BTZ solution. Sharif and Ama-Tul-Mughani [36] deformed both the metric functions to construct two anisotropic solutions from a known Tolman IV and Krori-Barua perfect fluid source. Similarly, Sharif and Saba [37] studied salient features of the resulted anisotropic solutions in  $f(G)$  gravity using Tolman IV as seed sector.

## 2 Essence of $f(G, T)$ Theory

In  $f(G, T)$  gravity, the action integral to formulate the field equations is given as

$$\mathbb{S}_{f(G,T)} = \int \left[ \frac{R + f(G, T)}{16\pi} + \mathcal{L}_m + \alpha \mathcal{L}_\delta \right] \sqrt{-g} d^4x, \quad (1)$$

where  $g$  denotes the determinant of the metric tensor and  $\mathcal{L}_m$  stands for the matter Lagrangian density. Here, the matter lagrangian density is taken as the positive pressure [38] and  $\mathcal{L}_\delta$  denotes the Lagrangian density corresponding to the extra sector. The relationships defining the lagrangian densities with their EMT sources are as follows

$$T_{\zeta\sigma} = g_{\zeta\sigma} \mathcal{L}_m - \frac{2\partial \mathcal{L}_m}{\partial g^{\zeta\sigma}}, \quad \delta_{\zeta\sigma} = g_{\zeta\sigma} \mathcal{L}_\delta - \frac{2\partial \mathcal{L}_\delta}{\partial g^{\zeta\sigma}}. \quad (2)$$

Here, the action (1) is varied with respect to the metric tensor to develop the field equations corresponding to  $f(G, T)$  gravity in the following form

$$G_{\zeta\sigma} = 8\pi T_{\zeta\sigma}^{(\text{tot})} = 8\pi(T_{\zeta\sigma}^{(\text{Cor})} + T_{\zeta\sigma}^{(\text{M})} + \alpha\delta_{\zeta\sigma}), \quad (3)$$

where  $\alpha$  expresses the decoupling parameter and  $G_{\zeta\sigma} = R_{\zeta\sigma} - \frac{1}{2}Rg_{\zeta\sigma}$  represents the Einstein tensor. The extra gravitational source  $\delta_{\zeta\sigma}$  induces anisotropy in the current configuration, and decoupling parameter  $\alpha$  connects the seed and additional sectors. Moreover, the extra curvature terms of  $f(G, T)$  theory read

$$\begin{aligned} T_{\zeta\sigma}^{(\text{Cor})} = & \frac{1}{8\pi} \left[ \{(p + \rho)v_{\zeta}v_{\sigma}\}f_T(G, T) + \frac{g_{\zeta\sigma}f(G, T)}{2} + (4R^{\mu\nu}R_{\zeta\mu\sigma\nu} \right. \\ & - 2RR_{\zeta\sigma} - 2R_{\zeta}^{\mu\nu\gamma}R_{\sigma\mu\nu\gamma} + 4R_{\mu\sigma}R_{\zeta}^{\mu}f_G(G, T) + (4g_{\zeta\sigma}R^{\mu\nu}\nabla_{\mu}\nabla_{\nu} \\ & - 4R_{\zeta}^{\mu}\nabla_{\sigma}\nabla_{\mu} - 4R_{\zeta\mu\sigma\nu}\nabla^{\mu}\nabla^{\nu} - 2g_{\zeta\sigma}R\nabla^2 + 2R\nabla_{\zeta}\nabla_{\sigma} - 4R_{\sigma}^{\mu}\nabla_{\zeta}\nabla_{\mu} \\ & \left. + 4R_{\zeta\sigma}\nabla^2)f_G(G, T) \right], \quad (4) \end{aligned}$$

where the d' Alembert operator is indicated by  $\square = \nabla^a\nabla_a = \nabla^2$  and  $\Theta_{\zeta\sigma} = -2T_{\zeta\sigma} + pg_{\zeta\sigma}$ . The partial derivatives of  $f(G, T)$  with respect to  $G$  and  $T$  are denoted by  $f_G = \frac{\partial f(G, T)}{\partial G}$  and  $f_T = \frac{\partial f(G, T)}{\partial T}$ , respectively. A consequential role is played by EMT to disclose the interior configuration of the self-gravitating entities. The EMT for the perfect matter source filled in the internal regime is described by

$$T_{\zeta\sigma}^{(\text{M})} = (\rho + p)v_{\zeta}v_{\sigma} + pg_{\zeta\sigma}, \quad (5)$$

where  $v_{\zeta}$  depicts the four-velocity satisfying the relation  $v^{\zeta}v_{\zeta} = -1$ ,  $p$  and  $\rho$  demonstrate the pressure and density, respectively.

The geometry under consideration is composed of inner and outer regions divided by the hypersurface. The internal spherically symmetric structure (static) is defined by the following metric

$$ds^2 = -e^{\varphi}dt^2 + e^{\vartheta}dr^2 + r^2(d\theta^2 + \sin^2\theta d\phi^2), \quad (6)$$

where both  $\varphi$  and  $\vartheta$  are functions of  $r$  solely. The velocity in terms of its components is written as

$$v^{\zeta} = \left( e^{-\frac{\varphi}{2}}, 0, 0, 0 \right). \quad (7)$$

For self-gravitating astrophysical objects, the modified field equations are

$$8\pi(\tilde{\rho} + T_0^{0(\text{Cor})} - \alpha\delta_0^0) = \frac{1}{r^2} + e^{-\vartheta}\left(\frac{\vartheta'}{r} - \frac{1}{r^2}\right), \quad (8)$$

$$8\pi(\tilde{p} + T_1^{1(\text{Cor})} + \alpha\delta_1^1) = -\frac{1}{r^2} + e^{-\vartheta}\left(\frac{1}{r^2} + \frac{\varphi'}{r}\right), \quad (9)$$

$$8\pi(\tilde{p} + T_2^{2(\text{Cor})} + \alpha\delta_2^2) = e^{-\vartheta}\left(\frac{\varphi'^2}{4} + \frac{\varphi''}{2} - \frac{\vartheta'\varphi'}{4} - \frac{\vartheta'}{2r} + \frac{\varphi'}{2r}\right), \quad (10)$$

where the derivative with respect to  $r$  is specified by prime and

$$\tilde{\rho} = p + \frac{\psi}{16\pi}(-\rho + 3p), \quad \tilde{p} = \rho + \frac{\psi}{16\pi}(3\rho - p), \quad (11)$$

correction terms  $T_0^{0(\text{Cor})}$ ,  $T_1^{1(\text{Cor})}$  and  $T_2^{2(\text{Cor})}$  are exhibited in Appendix **A** (Eqs.(A1)-(A3)).

The extra force exists because the EMT is not conserved in this theory. Meanwhile, the non-conservation of matter configuration is characterized by the following equation

$$\nabla^\varsigma T_{\varsigma\sigma} = \frac{f_T(G, T)}{8\pi - f_T(G, T)} \left[ \nabla^\varsigma \Theta_{\varsigma\sigma} - \frac{1}{2} g_{\varsigma\sigma} \nabla^\varsigma T + (\Theta_{\varsigma\sigma} + T_{\varsigma\sigma}) \nabla^\varsigma (\ln f_T(G, T)) \right],$$

which is left with the non-zero term

$$\frac{dp}{dr} + \frac{\vartheta'}{2}(p + \rho) + \alpha \frac{d\delta_1^1}{dr} + \frac{2\alpha}{r}(\delta_1^1 - \delta_2^2) + \frac{\alpha\vartheta'}{2}(\delta_1^1 - \delta_0^0) = \Gamma, \quad (12)$$

where  $\Gamma$  includes the modified terms as

$$\Gamma = \frac{\psi}{8\pi - \psi} \left[ -\frac{(-\rho + 3p)'}{2} - \alpha\delta_1^1 (\ln f_T)' + (-2p)' \right]. \quad (13)$$

Here, it is important to note that a successful decoupling is achieved in EGD approach when the exchange of energy between normal matter and extra source happens. The following explicit  $f(G, T)$  theory model [39] is used to explore the viable and stable anisotropic solutions

$$f(G, T) = \mathfrak{f}_1(G) + \mathfrak{f}_2(T), \quad (14)$$

where  $\mathfrak{f}_1$  and  $\mathfrak{f}_2$  are separately defined functions of  $G$  and  $T$ , respectively. In this curvature-matter coupled theory, we select a quadratic model to analyze

its role in understanding the physical features of the stellar structure. Hence,  $\mathbf{f}_1(G) = \chi G^2$  and  $\mathbf{f}_2(T) = \psi T$  are fixed, where  $\psi$  and  $\chi$  are free parameter and real constant, respectively. The expressions of  $G$  along with its higher derivatives are exhibited in Eqs.(A4)-(A6) of Appendix A.

The non-linear differential Eqs.(8)-(10) as well as (12) form a system with seven unknown quantities ( $\varphi, \vartheta, \rho, p, \delta_0^0, \delta_1^1, \delta_2^2$ ), indicating that the system has fewer equations than unknown parameters. Thus, to close the system more constraints are required. For this purpose, we use a systematic scheme of EGD to obtain the solution of our system. The matter variables are easily identified as

$$\check{\rho} = \rho - \alpha\delta_0^0, \quad \check{p}_r = p + \alpha\delta_1^1, \quad \check{p}_t = p + \alpha\delta_2^2. \quad (15)$$

The above expressions assure that the anisotropy is induced due to the extra source ( $\delta_\sigma^\xi$ ) within self-gravitating system. Thus, when  $\delta_1^1 \neq \delta_2^2$ , the effective anisotropy becomes

$$\check{\Delta} = \check{p}_t - \check{p}_r = \alpha(\delta_2^2 - \delta_1^1). \quad (16)$$

### 3 Extended Gravitational Decoupling Scheme

In this section, a novel approach entitled as gravitational decoupling by means of EGD is utilized to determine the unknowns by resolving the system (8)-(10). According to this method, the field equations are segregated such that the anisotropy produced in the internal structure is caused by the presence of extra source ( $\delta_\sigma^\xi$ ). For this purpose, we consider the following metric for perfect matter source

$$ds^2 = \frac{dr^2}{\epsilon(r)} - e^{\xi(r)} dt^2 + r^2 d\theta^2 + r^2 \sin^2 \theta d\phi^2, \quad (17)$$

where  $\epsilon(r) = 1 - \frac{2m}{r}$ ,  $m(r)$  conforms the Misner-Sharp mass of the inner celestial structure. The effects of anisotropy on the perfect source are encoded by implementing the linear geometrical transformation to temporal as well as radial metric components through

$$\xi \rightarrow \varphi = \xi + \alpha h^*, \quad \epsilon \rightarrow e^{-\vartheta(r)} = \epsilon + \alpha k^*, \quad (18)$$

where  $k^*$  and  $h^*$  are the deformation functions associated to radial and temporal metric potentials, respectively, and  $\alpha$  participates in governing the



working of both deformations. These decompositions divide the field equations (8)-(10) into two arrays, in which the first set represents the perfect source ( $\alpha = 0$ ) as

$$8\pi(\rho + \frac{\psi}{16\pi}(3\rho - p) + T_0^{0(\text{Cor})}) = \frac{1}{r^2} - (\frac{\epsilon'}{r} + \frac{\epsilon}{r^2}), \quad (19)$$

$$8\pi(p + \frac{\psi}{16\pi}(-\rho + 3p) + T_1^{1(\text{Cor})}) = -\frac{1}{r^2} + \frac{\epsilon}{r}(\frac{1}{r} + \xi'), \quad (20)$$

$$8\pi(p + \frac{\psi}{16\pi}(-\rho + 3p) + T_2^{2(\text{Cor})}) = \epsilon(\frac{\xi''}{2} + \frac{\xi'^2}{4} + \frac{\xi'}{2r}) + \epsilon'(\frac{\xi'}{4} + \frac{1}{2r}). \quad (21)$$

Solving the above equations, we obtain density and pressure for the isotropic sector as

$$\rho = \frac{-1}{4(\psi^2 + 12\pi\psi + 32\pi^2)r^2} \left( -2\psi + 3\psi r^2 T_0^{0(\text{Cor})} + 16\pi r^2 T_0^{0(\text{Cor})} + \psi r^2 T_1^{1(\text{Cor})} + 3\psi r \epsilon' - \psi r \epsilon \xi' + 2\psi \epsilon + 16\pi r \epsilon' + 16\pi \epsilon - 16\pi \right), \quad (22)$$

$$p = \frac{-1}{4(\psi^2 + 12\pi\psi + 32\pi^2)r^2} \left( 2\psi + \psi r^2 T_0^{0(\text{Cor})} + 3\psi r^2 T_1^{1(\text{Cor})} + 16\pi r^2 T_1^{1(\text{Cor})} + \psi r \epsilon' - 3\psi r \epsilon \xi' - 2\psi \epsilon - 16\pi r \epsilon \xi' - 16\pi \epsilon + 16\pi \right), \quad (23)$$

whereas the induced anisotropy due to new sector is evaluated through the second set

$$8\pi\delta_0^0 = \frac{k^{*'}}{r} + \frac{k^*}{r^2}, \quad (24)$$

$$8\pi\delta_1^1 = \frac{\alpha k^* h^{*'}}{r} + \frac{\epsilon h^{*'}}{r} + \frac{k^*}{r^2} + \frac{k^* \xi'}{r}, \quad (25)$$

$$8\pi\delta_2^2 = \frac{k^{*'}(\alpha h^{*'} + \xi')}{4} + \frac{h^{*'} \epsilon'}{4} + k^* \left( \frac{(\alpha h^{*''} + \xi'')}{2} + \frac{(\alpha h^{*'} + \xi')^2}{4} + \frac{\alpha h^{*'} + \xi'}{2r} \right) + \frac{k^{*'}}{2r} + \epsilon \left( \frac{h^{*''}}{2} + \frac{\alpha h^{*'^2}}{4} + \frac{h^{*'} \xi'}{2} + \frac{h^{*'}}{2r} \right). \quad (26)$$

It should be noticed that the system (19)-(21) is comprised of four unknowns, i.e.,  $p, \rho, \xi$  and  $\epsilon$ , while the anisotropic set (24)-(26) contains nine unknowns

$(\rho, p, \xi, \epsilon, \delta_0^0, \delta_1^1, \delta_2^2, k^*, h^*)$ . Thus we need to specify the isotropic set so that we might be able to determine the solution corresponding to anisotropic sector. Consequently, the number of unknowns will be reduced from seven to five, indicating that the EGD technique assists in developing the anisotropic solutions.

## 4 Interior Anisotropic Solutions

Now, we study anisotropic solutions of the astrophysical object through some definite forms of the isotropic set. For this purpose, we take the Krori-Barua metric [40] as seed (isotropic) solution which is attributed to singularity-free nature. The metric coefficients are defined as

$$e^{\xi(r)} = e^{Lr^2+P}, \quad e^{\vartheta(r)} = \epsilon^{-1} = e^{Xr^2}. \quad (27)$$

Consequently, the values of  $\rho$  and  $p$  from Eqs.(19)-(21) in terms of the above mentioned potentials become

$$\rho = \frac{e^{-r^2X}}{4(\psi^2 + 12\pi\psi + 32\pi^2)r^2} \left( (-\psi(-2Lr^2 + e^{r^2X}(r^2(3T_0^{0(\text{Cor})} + T_1^{1(\text{Cor})}) - 2) - 6r^2X + 2) - 16\pi((r^2T_0^{0(\text{Cor})} - 1)e^{r^2X} - 2r^2X + 1)) \right), \quad (28)$$

$$p = \frac{e^{-r^2X}}{4(\psi^2 + 12\pi\psi + 32\pi^2)r^2} \left( (-\psi(e^{r^2X}(r^2(T_0^{0(\text{Cor})} + 3T_1^{1(\text{Cor})}) + 2) - 2(3Lr^2 + r^2X + 1)) - 16\pi(-2Lr^2 + (r^2T_1^{1(\text{Cor})} + 1)e^{r^2X} - 1)) \right). \quad (29)$$

The junction conditions help to determine the unknown constants  $(L, P, X)$  involved in the above equations. When the interior and exterior structures are matched over the hypersurface, the continuity of metric potentials give the constants as

$$L = \frac{M_o R}{R^4 \left(1 - \frac{2M_o}{R}\right)}, \quad (30)$$

$$P = \frac{R^2 \left(1 - \frac{2M_o}{R}\right) \ln \left(1 - \frac{2M_o}{R}\right) - M_o R}{R^2 \left(1 - \frac{2M_o}{R}\right)}, \quad (31)$$

$$X = \frac{1}{R^2} \ln \left( \frac{1}{1 - \frac{2M_o}{R}} \right). \quad (32)$$

together with  $\frac{M_o}{R} < \frac{4}{9}$ ,  $M_o$  denotes the mass at the boundary. The compatibility of isotropic solution (28) and (29) with the Schwarzschild at the junction is assured by the above-mentioned equations that can be altered in the internal regime with the addition of extra source. The radial and temporal coefficients (Eq.(27)) will help to evaluate the anisotropic solutions. The deformation functions  $h^*$  and  $k^*$  are related to the source term in (24)-(26). The solution of this system is evaluated by implying certain constraints. As this system constitutes five unknowns and three equations, therefore, we require two more constraints to close the system. We utilize the linear equation of state on  $\delta_\sigma^s$  as

$$\delta_0^0 = a\delta_1^1 + b\delta_2^2. \quad (33)$$

For the sake of simplicity, we substitute  $a = 1$  and  $b = 0$ , hence, the above equation will become  $\delta_0^0 = \delta_1^1$ . Furthermore, we use the astrophysical object 4U 1820-30 [41] whose mass and radius are  $1.58 \pm 0.06M_\odot$  and  $9.1 \pm 0.4\text{km}$ , respectively.

In the subsequent sections, we implement some limitations to develop two interior anisotropic solutions and will then analyze their graphical behavior.

## 4.1 The First Solution

The system (24)-(26) is closed by imposing an additional condition on the radial part of the new source together with the equation of state. These two constraints are utilized to determine the deformation functions ( $h^*$ ,  $k^*$ ) which are further employed in formulating the components of  $\delta_\sigma^s$ . It can be noticed that the inner configuration depicts the consistency with outer distribution as far as  $\tilde{p}(R) + T_1^{1(\text{Cor})}(R) \sim \alpha(\delta_1^1(R))_-$  holds. This requirement is fulfilled by using [26]

$$\tilde{p} + T_1^{1(\text{Cor})} = \delta_1^1. \quad (34)$$

By utilizing the metric coefficients (27) in the field equations (20),(24) and (25), the deformation functions become

$$h^* = \int \left\{ \sqrt{\pi}(2Lr^2 + 1)(L + X)e^{r^2X} \text{Erf}(r\sqrt{X}) - 2r\sqrt{X}(2L^2r^2 + L(2r^2X + 1) + X) \right\} \left\{ r(2r\sqrt{X}(\alpha L + X(\alpha e^{r^2X} - 1)) - \sqrt{\pi}\alpha(L + X)) \right.$$

$$e^{r^2 X} \text{Erf}(r\sqrt{X})\}^{-1} dr, \quad (35)$$

$$k^* = \frac{\sqrt{\pi}(L+X)\text{Erf}(r\sqrt{X})}{2rX^{3/2}} - \frac{Le^{-r^2 X} + X}{X}. \quad (36)$$

These deformation functions help to compose the temporal and radial potentials as

$$\begin{aligned} \varphi &= Lr^2 + P + \alpha \int \left\{ \sqrt{\pi}(2Lr^2 + 1)(L+X)e^{r^2 X} \text{Erf}(r\sqrt{X}) - 2r\sqrt{X}(2L^2r^2 \right. \\ &\quad \left. + L(2r^2 X(e^{r^2 X} + 1) + 1) + X) \right\} \left\{ r(2r\sqrt{X}(\alpha L + X(\alpha e^{r^2 X} - 1)) \right. \\ &\quad \left. - \sqrt{\pi}\alpha(L+X)e^{r^2 X} \text{Erf}(r\sqrt{X})) \right\}^{-1} dr, \quad (37) \\ e^{-\vartheta} &= -\alpha + \frac{\sqrt{\pi}\alpha(L+X)\text{Erf}(r\sqrt{X})}{2rX^{3/2}} + \frac{e^{-r^2 X}(X - \alpha L)}{X}, \end{aligned}$$

and for  $\alpha = 0$ , this yields the standard Krori-Barua solution for perfect source.

We employ the junction conditions to examine the effect of anisotropy on  $L, P$  and  $X$ . Thus, the first fundamental form of matching conditions yields the following results

$$\begin{aligned} \ln \left( 1 - \frac{M_o}{R} \right) &= LR^2 + P + \alpha \left[ \int \left\{ \sqrt{\pi}(2Lr^2 + 1)(L+X)e^{r^2 X} \text{Erf}(r\sqrt{X}) \right. \right. \\ &\quad \left. \left. - 2r\sqrt{X}(2L^2r^2 + L(2r^2 X(e^{r^2 X} + 1) + 1) + X) \right\} \left\{ r(2r\sqrt{X} \right. \right. \\ &\quad \left. \left. (\alpha L + X(\alpha e^{r^2 X} - 1)) - \sqrt{\pi}\alpha(L+X)e^{r^2 X} \text{Erf}(r\sqrt{X})) \right\}^{-1} dr \right]_{r=R}, \quad (38) \end{aligned}$$

$$1 - \frac{M_o}{R} = \frac{\sqrt{\pi}\alpha(L+X)\text{Erf}(R\sqrt{X})}{2RX^{3/2}} + \frac{e^{-R^2 X}(X - \alpha L)}{X} - \alpha. \quad (39)$$

In the same way, the second fundamental form  $(\tilde{p}(R) + T_1^{1(\text{Cor})}(R) - \alpha(\delta_1^1(R))_- = 0)$  gives

$$X = \frac{\ln(1 + 2LR^2)}{R^2}. \quad (40)$$

The necessary and sufficient conditions to match the interior and exterior geometries at the junction are provided by Eqs.(38)-(40). The expressions of first anisotropic solution and anisotropic factor corresponding to (33) and

(34) are

$$\begin{aligned} \check{\rho} = \frac{e^{-r^2X}}{8r^2} & \left[ \frac{1}{\psi^2 + 12\pi\psi + 32\pi^2} \left\{ -2\psi(-2Lr^2 + e^{r^2X}(r^2(3T_0^{0(\text{Cor})} + T_1^{1(\text{Cor})}) \right. \right. \\ & \left. \left. - 2) - 6r^2X + 2) - 32\pi((r^2T_0^{0(\text{Cor})} - 1)e^{r^2X} - 2r^2X + 1) \right\} + \frac{1}{\pi} \left\{ \alpha(-2Lr^2 \right. \\ & \left. + e^{r^2X} - 1) \right\} \right], \end{aligned} \quad (41)$$

$$\begin{aligned} \check{\rho}_r = \frac{e^{-r^2X}}{8r^2} & \left[ \frac{1}{\psi^2 + 12\pi\psi + 32\pi^2} \left\{ -2\psi(e^{r^2X}(r^2(T_0^{0(\text{Cor})} + 3T_1^{1(\text{Cor})}) + 2) - 2(3Lr^2 \right. \right. \\ & \left. \left. + r^2X + 1)) - 32\pi(-2Lr^2 + (r^2T_1^{1(\text{Cor})} + 1)e^{r^2X} - 1) \right\} + \frac{1}{\pi} \left\{ \alpha(2Lr^2 + 1 \right. \\ & \left. - e^{r^2X}) \right\} \right], \end{aligned} \quad (42)$$

$$\begin{aligned} \check{\rho}_t = \frac{1}{16}e^{-r^2X} & \left[ \left\{ \alpha(2r\sqrt{X}(2L^3r^2 + L^2(-4\alpha + 2r^2X(2\alpha + e^{r^2X} + 2) + 1) \right. \right. \\ & \left. \left. + 2LX(\alpha + r^2X((2\alpha + 1)e^{r^2X} - 1) - 2\alpha e^{r^2X} + 3) + X^2(2\alpha e^{r^2X} - 1)) \right. \right. \\ & \left. \left. - \sqrt{\pi}(L + X)e^{r^2X}\text{Erf}(r\sqrt{X})(2L^2r^2 + L(-4\alpha + 2r^2(2\alpha X + X) + 1) \right. \right. \\ & \left. \left. + 2\alpha X + X) \right\} \left\{ \pi(\sqrt{\pi}\alpha(L + X)e^{r^2X}\text{Erf}(r\sqrt{X}) - 2r\sqrt{X}(\alpha L + X(\alpha e^{r^2X} \right. \right. \\ & \left. \left. - 1))) \right\}^{-1} - \left\{ 4(\psi(e^{r^2X}(r^2(T_0^{0(\text{Cor})} + 3T_1^{1(\text{Cor})}) + 2) - 2(3Lr^2 + r^2X + 1)) \right. \right. \\ & \left. \left. + 16\pi(-2Lr^2 + (r^2T_1^{1(\text{Cor})} + 1)e^{r^2X} - 1)) \right\} \left\{ (\psi^2 + 12\pi\psi + 32\pi^2)r^2 \right\}^{-1} \right], \end{aligned} \quad (43)$$

$$\begin{aligned} \check{\Delta} = & \left\{ \alpha e^{-r^2X}(-\sqrt{\pi}(L + X)e^{r^2X}\text{Erf}(r\sqrt{X})(-2L^2r^4 - L(2r^4(2\alpha X + X) \right. \right. \\ & \left. \left. + r^2) - r^2(2\alpha X + X) + 2\alpha(e^{r^2X} - 1)) - 2r\sqrt{X}(2L^3r^4 + L^2(r^2 + 2r^4X \right. \right. \\ & \left. \left. \times (2\alpha + e^{r^2X} + 2)) + 2L(\alpha + (\alpha + 1)r^2X - \alpha e^{r^2X} + r^4X^2((2\alpha + 1)e^{r^2X} \right. \right. \\ & \left. \left. - 1)) + X(-2\alpha e^{2r^2X} + 2e^{r^2X}(\alpha + \alpha r^2X + 1) + r^2(-X) - 2)) \right\} \\ & \times \left\{ 16\pi r^2(\sqrt{\pi}\alpha(L + X)e^{r^2X}\text{Erf}(r\sqrt{X}) - 2r\sqrt{X}(\alpha L + X(\alpha e^{r^2X} - 1))) \right\}^{-1}. \end{aligned} \quad (44)$$

## 4.2 The Second Solution

The second anisotropic solution is computed by utilizing a density-like constraint, i.e.,

$$\tilde{\rho} + T_0^{0(\text{Cor})} = \delta_0^0. \quad (45)$$

Making use of Eq.(19) along with (24) and (25), we have

$$h^* = \frac{(L + \alpha X) \ln(\alpha(e^{r^2 X} - 1) + 1) - \alpha r^2 X(L + X)}{(\alpha - 1)\alpha X}, \quad (46)$$

$$k^* = 1 - e^{-r^2 X}. \quad (47)$$

In this solution, the matching conditions are

$$\ln\left(1 - \frac{\mathbb{M}_o}{\mathbb{R}}\right) = \frac{(L + \alpha X) \ln(\alpha(e^{R^2 X} - 1) + 1) - \alpha R^2 X(L + X)}{(\alpha - 1)X} + P + LR^2, \quad (48)$$

$$1 - \frac{\mathbb{M}_o}{\mathbb{R}} = \alpha - (\alpha - 1)e^{-R^2 X}. \quad (49)$$

Finally, the matter variables for solution II are as follows

$$\begin{aligned} \check{\rho} = \frac{e^{-r^2 X}}{8r^2} & \left[ \frac{1}{\psi^2 + 12\pi\psi + 32\pi^2} \{ -2\psi(-2Lr^2 + e^{r^2 X}(r^2(3T_0^{0(\text{Cor})} + T_1^{1(\text{Cor})}) \right. \\ & - 2) - 6r^2 X + 2) - 32\pi((r^2 T_0^{0(\text{Cor})} - 1)e^{r^2 X} - 2r^2 X + 1)\} - \frac{1}{\pi} \{ \alpha(2r^2 X \\ & \left. + e^{r^2 X} - 1) \} \right], \end{aligned} \quad (50)$$

$$\begin{aligned} \check{p}_r = \frac{e^{-r^2 X}}{8r^2} & \left[ \frac{1}{\psi^2 + 12\pi\psi + 32\pi^2} \{ -2\psi(e^{r^2 X}(r^2(T_0^{0(\text{Cor})} + 3T_1^{1(\text{Cor})}) + 2) - 2(3L \right. \\ & \times r^2 + r^2 X + 1)) - 32\pi(-2Lr^2 + (r^2 T_1^{1(\text{Cor})} + 1)e^{r^2 X} - 1)\} + \frac{1}{\pi} \{ \alpha(2r^2 X \\ & \left. + e^{r^2 X} - 1) \} \right], \end{aligned} \quad (51)$$

$$\begin{aligned} \check{p}_t = \frac{1}{8} e^{-r^2 X} & \left[ \{ -2\psi(e^{r^2 X}(r^2(T_0^{0(\text{Cor})} + 3T_1^{1(\text{Cor})}) + 2) - 2(3Lr^2 + r^2 X + 1)) \right. \\ & - 32\pi(-2Lr^2 + (r^2 T_1^{1(\text{Cor})} + 1)e^{r^2 X} - 1)\} \{ (\psi^2 + 12\pi\psi + 32\pi^2)r^2 \}^{-1} \\ & \left. - \{ \alpha(L^2 r^2(e^{r^2 X} - 1) + Lr^2 X(e^{r^2 X} - 2) + X(3\alpha + r^2 X(2\alpha(e^{r^2 X} - 1) \right. \end{aligned}$$

$$+ 1) - 3\alpha e^{r^2 X} - 3))\}\{\pi(\alpha(e^{r^2 X} - 1) + 1)\}^{-1}]. \quad (52)$$

The anisotropic expression for this solution is

$$\begin{aligned} \check{\Delta} = & \{\alpha e^{-r^2 X} (\alpha - L^2 r^4 + e^{r^2 X} (L^2 r^4 + L r^4 X + \alpha(2r^4 X^2 - r^2 X - 2) + 1) \\ & - 2L r^4 X - 2\alpha r^4 X^2 + r^4 X^2 + \alpha r^2 X + \alpha e^{2r^2 X} - r^2 X - 1)\}\{8\pi r^2 (\alpha(e^{r^2 X} \\ & - 1) + 1)\}^{-1}. \end{aligned} \quad (53)$$

## 5 Essential Characteristics

This section investigates some feasible and stable features of the acquired anisotropic solutions. To do so, we consider the model (14) and choose the parameters  $\psi$  and  $\chi$  as -13 and 1, respectively. For solution I, the positive values of  $\psi$  correspond to the acceptable behavior of matter variables and energy constraints. However, all the physical tests fail to check the stability of the first solution (not plotted here). This leads us to select the negative value of  $\psi$  as -13 for both solutions. This value of coupling parameter shows acceptable behavior of state variables, energy conditions and stability criteria corresponding to both solutions. We can thus deduce that the negative value of  $\psi$  provides compatible solutions, while positive values produce the encounter behavior. Moreover, this leads to the fact that the positive  $\psi$  does not yield consistent results and hence cannot discuss the self-gravitating bodies.

The constant terms (L and P) are interpreted from (30) and (31) whereas X is selected from (40). The feasibility of the compact structure is checked through the behavior of effective matter distributions. The effective energy density and pressure ingredients should be maximum, finite as well as positive near the center and must decrease with an increment in  $r$ . For solution I, the plots of density and anisotropic pressures in Figure 1 illustrate the maximal trend near the center and then show monotonic decreasing behavior towards the boundary with  $r$ . It is also seen that the tangential/radial pressures at the surface of star are zero. The last plot of Figure 1 shows that anisotropy disappears at the center while it becomes paramount on reaching the boundary. One can also examine that anisotropy is zero at the center for all values of the decoupling parameter, whereas at the stellar surface, the anisotropy increases by increasing  $\alpha$  which assures that the extra source

generates anisotropy in the system. To examine the internal realistic fluid of the compact object, some bounds are imposed on the EMT, known as energy conditions. These constraints guarantee the existence of normal matter and viability of the developed solutions. Four energy conditions, i.e., weak (WEC), null (NEC), dominant (DEC) and strong (SEC) for anisotropic configuration are specified as

$$\begin{aligned}
\text{NEC: } & \check{\rho} + \check{p}_r \geq 0, \quad \check{\rho} + \check{p}_t \geq 0, \\
\text{WEC: } & \check{\rho} + \check{p}_t \geq 0, \quad \check{\rho} \geq 0, \quad \check{\rho} + \check{p}_r \geq 0, \\
\text{DEC: } & \check{\rho} - \check{p}_t \geq 0, \quad \check{\rho} - \check{p}_r \geq 0, \\
\text{SEC: } & \check{\rho} + \check{p}_r + 2\check{p}_t \geq 0.
\end{aligned} \tag{54}$$

Stability of a compact structure is a crucial factor to examine the physical acceptability of the derived models. There are different methods to gauge the stable structure of celestial object. One of the techniques is causality condition, which states that the speed of light must always be faster than the speed of sound. The components of the speed sound are represented as

$$\nu_t^2 = \frac{d\check{p}_t}{d\check{\rho}}, \quad \nu_r^2 = \frac{d\check{p}_r}{d\check{\rho}}, \tag{55}$$

where  $\nu_t^2$  and  $\nu_r^2$  are the tangential and radial square speed components, respectively, with  $0 < \nu_t^2 < 1$  as well as  $0 < \nu_r^2 < 1$  [42]. Another way to determine the stability is proposed by Herrera [43], i.e., cracking approach according to which the constituents of sound speed associated with the stellar system should lie in  $|\nu_t^2 - \nu_r^2| < 1$ . The adiabatic index is an alternative technique which supports the stable behavior of astronomical objects defined as

$$\check{\Gamma}_r = \frac{\check{\rho} + \check{p}_r}{\check{p}_r} \left( \frac{d\check{p}_r}{d\check{\rho}} \right), \quad \check{\Gamma}_t = \frac{\check{\rho} + \check{p}_t}{\check{p}_t} \left( \frac{d\check{p}_t}{d\check{\rho}} \right). \tag{56}$$

The astrophysical structure shows the stable region if radial as well as tangential part of adiabatic index is greater than  $\frac{4}{3}$  [44]. Figure **2** indicates that all the energy conditions for the first solution comply with the required limits, so the solution I is viable. It is also clear from Figure **3** that the first solution meets the requirements of all three stability criteria, which indicates the stability of solution I.

The physical analysis of the second solution is accomplished by considering the same values as chosen in solution I. The matter determinants,



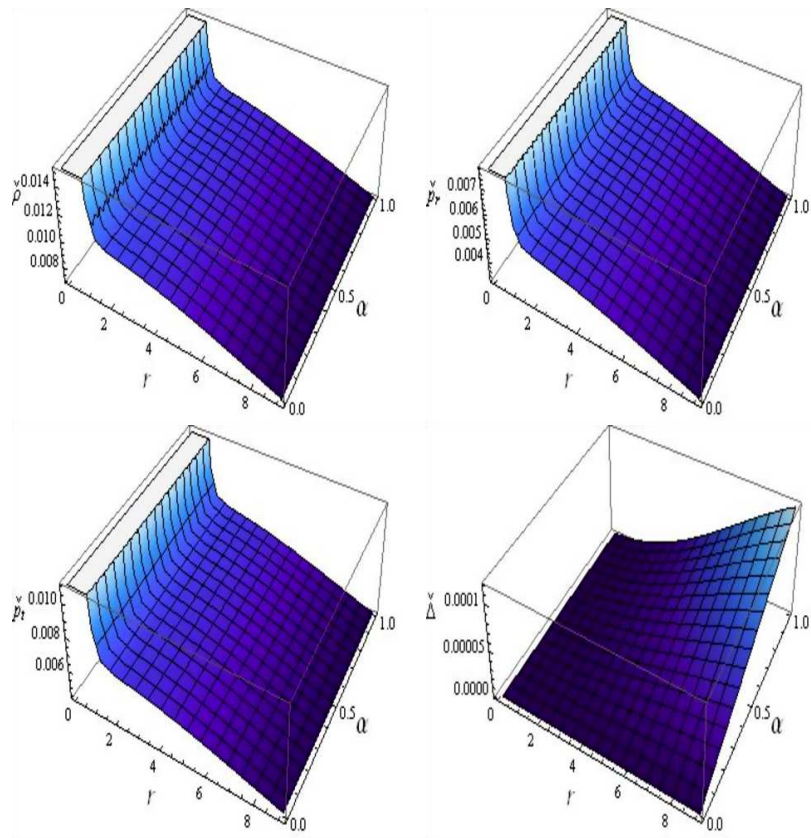


Figure 1: Analysis of  $\check{\rho}, \check{p}_r, \check{p}_t$  (density and pressure components) and  $\check{\Delta}$  (anisotropy) versus  $r$  and  $\alpha$  for the solution I.

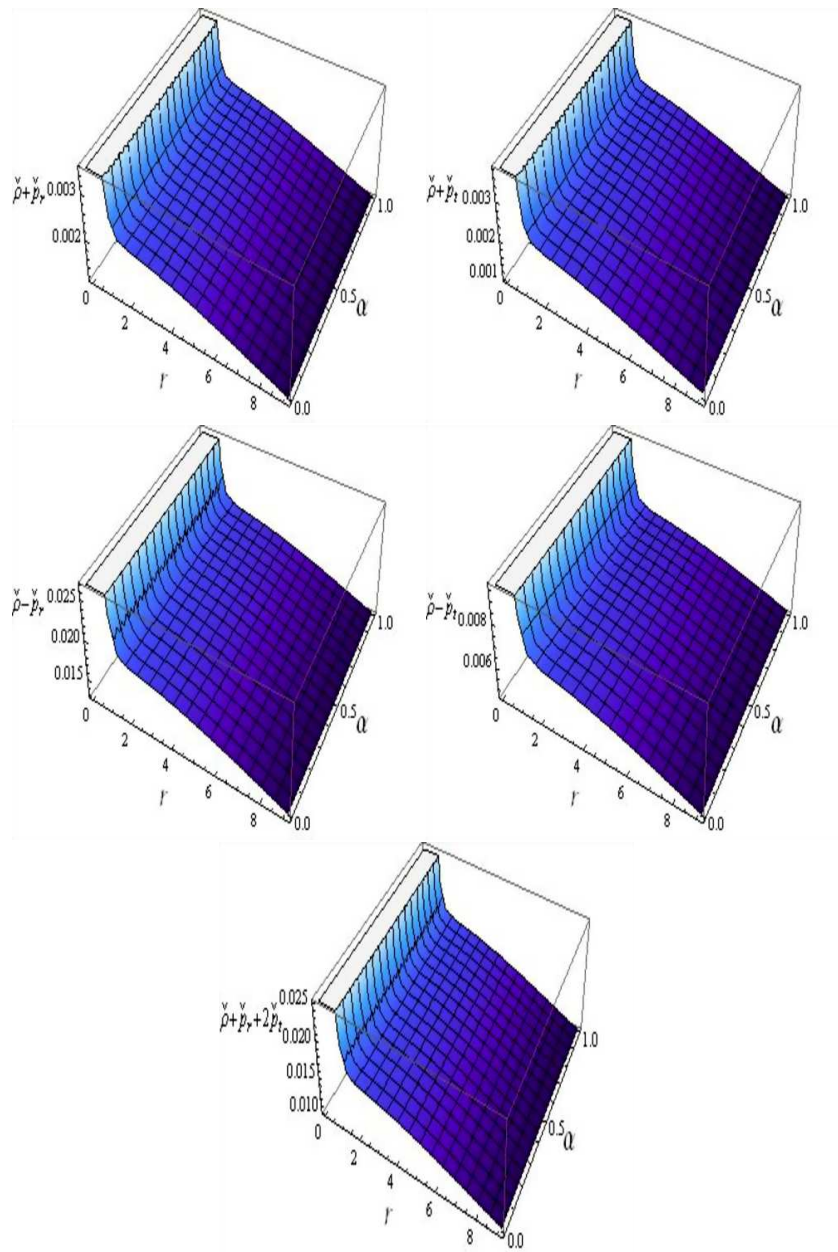


Figure 2: Analysis of energy constraints for the solution I.

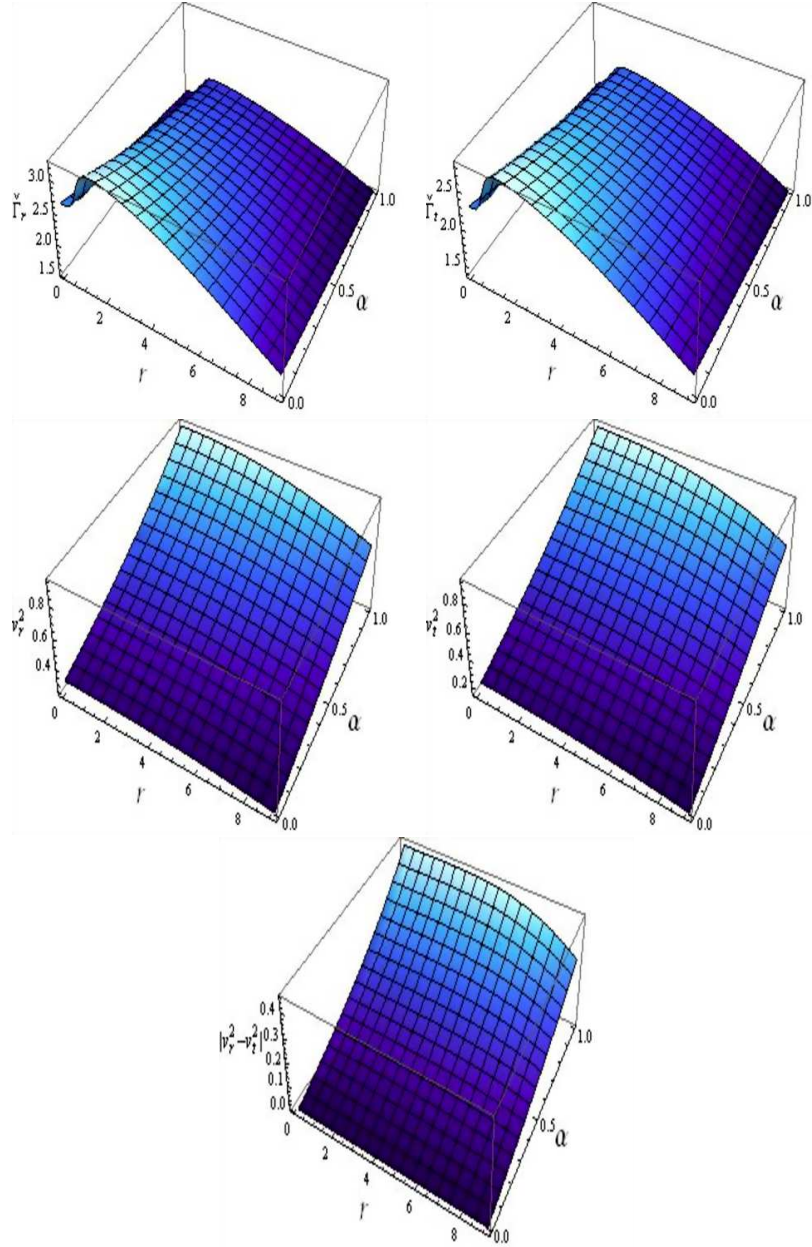


Figure 3: Analysis of adiabatic index, causality condition and Herrera cracking approach versus  $r$  and  $\alpha$  for the solution I.

likewise in solution I, must be finite, maximum and decreasing with  $r$ . The energy density, radial/tangential pressures in Figure 4 are maximum near the center and decline towards the boundary as  $r$  increases. The graphical representation of anisotropy in Figure 4 exhibits zero behavior at the center and persists this behavior throughout  $r$ . It is also observed that for all values of  $\alpha$ , anisotropy becomes zero at the core while it displays an increment at the star surface with larger values of the decoupling parameter. The viability of solution II is shown in Figure 5 as energy constraints are satisfied. Figure 6 shows the stable behavior of solution II through both causality condition as well as Herrera cracking approach. Moreover, the adiabatic index is also validated in the whole domain since its radial and tangential components lie within the stable range (Figure 6). Hence, solution II demonstrates the stable behavior according to all the criteria.

The mass of static spherically symmetric distribution is computed by

$$m = 4\pi \int_0^R \check{\rho} r^2 dr. \quad (57)$$

The numerical approach is utilized in Eq.(57) with the initial condition  $m(0) = 0$  to calculate the mass of anisotropic celestial object. One of the substantial features of an astrophysical object is its compactness ( $\zeta$ ), which is defined as the ratio between mass and radius of the considered star. The upper limit of compactness is calculated by Buchdahl [45] by matching the inner geometry with the outer Schwarzschild vacuum regime through junction conditions. This limit is found to be less than  $\frac{4}{9}$  for stable stellar configurations. The electromagnetic radiations are produced by the celestial objects whose wavelength is enlarged due to strong gravitational pull, thus this increment in wavelength is analyzed by redshift parameter ( $Z(r) = \frac{1}{\sqrt{1-2\zeta}} - 1$ ). Buchdahl found this factor as  $Z(r) < 2$  for isotropic source but 5.211 for anisotropic matter [46].

In order to investigate the mass, compactness and redshift factor for solutions I and II, we select four values of the decoupling parameter, i.e.,  $\alpha = 0.01, 0.25, 0.55, 0.85$ . Figure 7 represents that mass, compactness and redshift parameters slightly decrease for larger values of  $\alpha$  (solution I). For the solution II, one can notice a significant decline in mass, compactness as well as redshift factor for higher values of the decoupling parameter (Figure 8). The components of the equation of state parameter of anisotropic

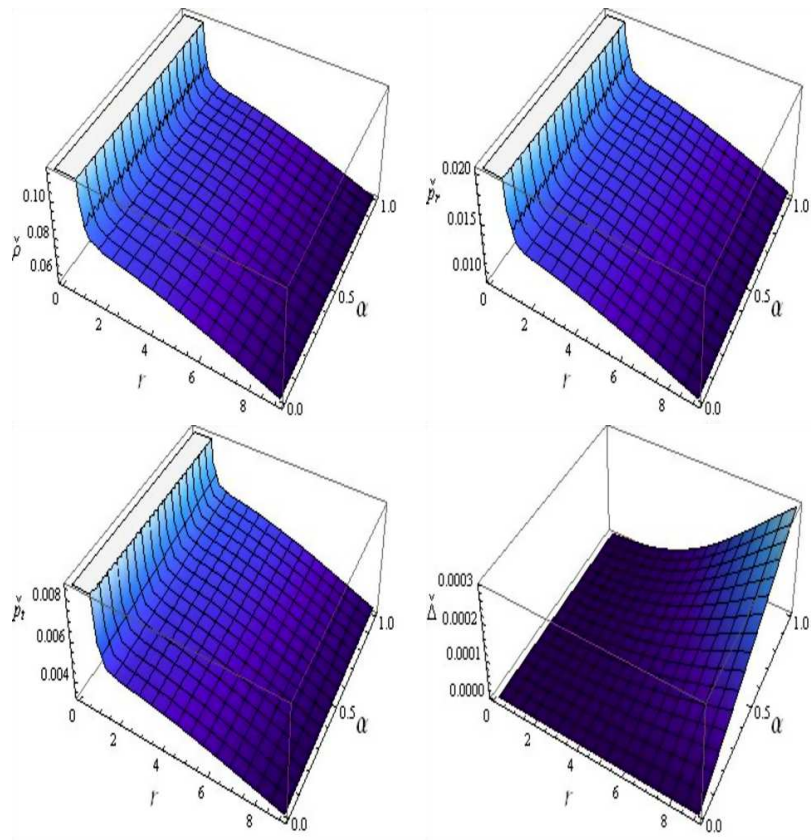


Figure 4: Analysis of  $\check{\rho}, \check{p}_r, \check{p}_t$  (density and pressure components) and  $\check{\Delta}$  (anisotropy) versus  $r$  and  $\alpha$  for the solution II.

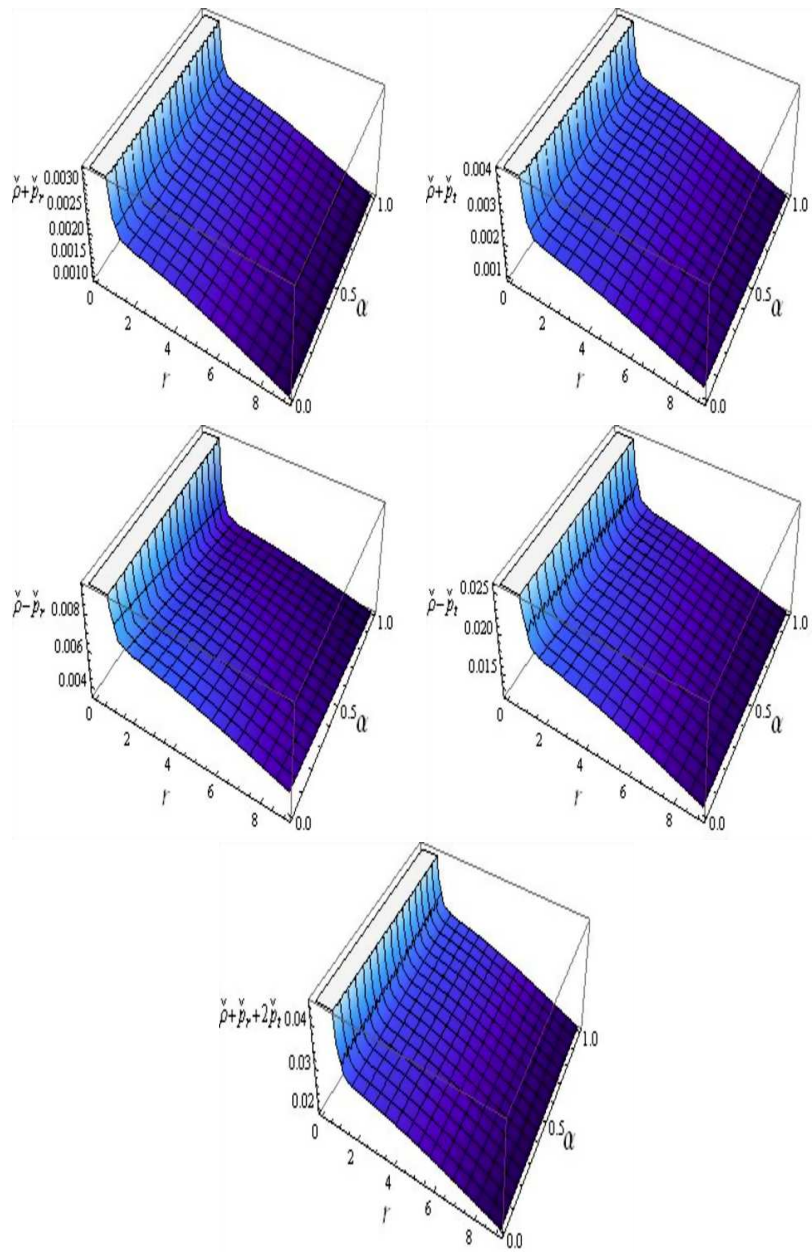


Figure 5: Analysis of energy constraints for the solution II.

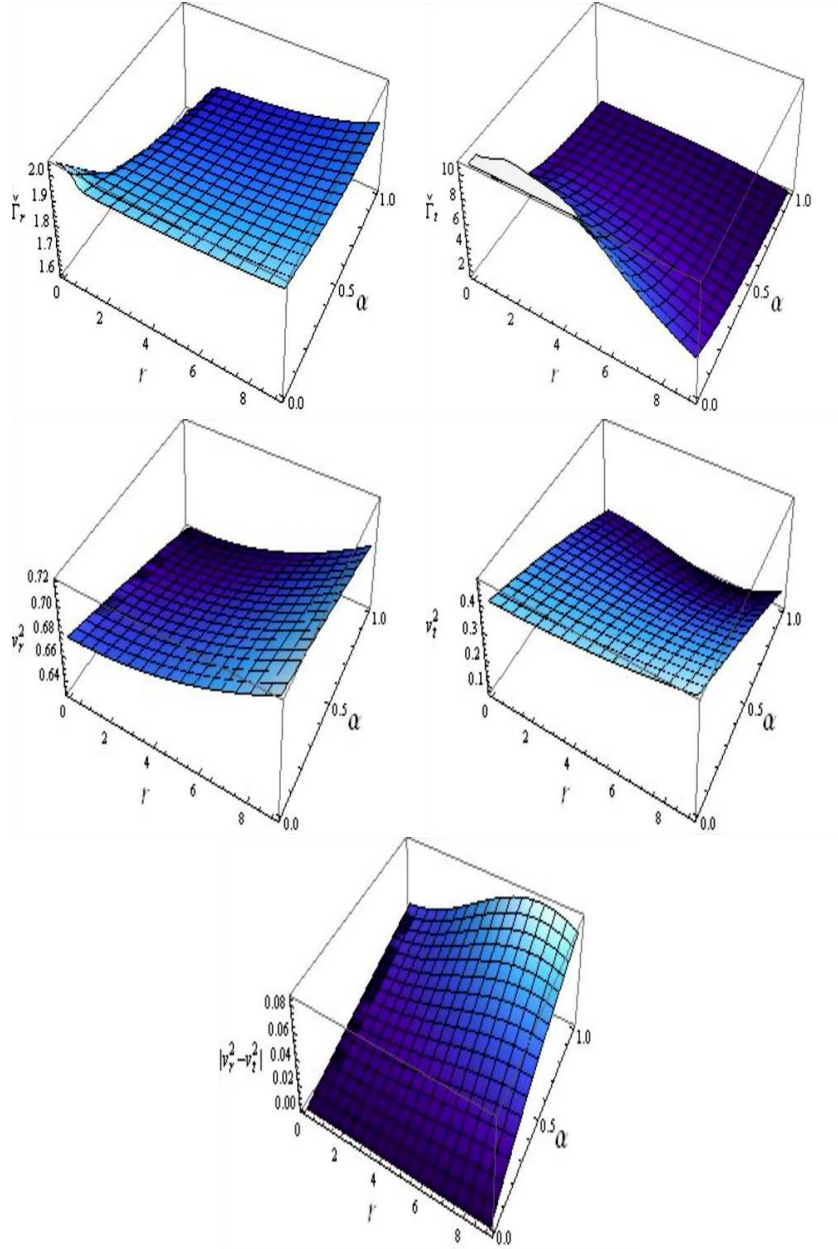


Figure 6: Analysis of adiabatic index, causality condition and Herrera cracking approach versus  $r$  and  $\alpha$  for the solution II.

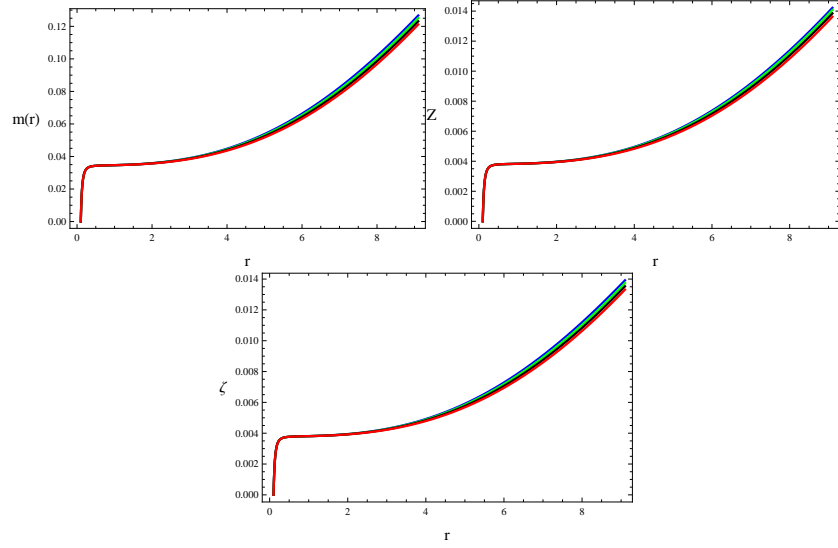


Figure 7: Behavior of mass, redshift and compactness versus  $r$  corresponding to  $\alpha = 0.01$  (Blue),  $0.25$  (Green),  $0.55$  (Black) and  $0.85$  (Red) for solution I.

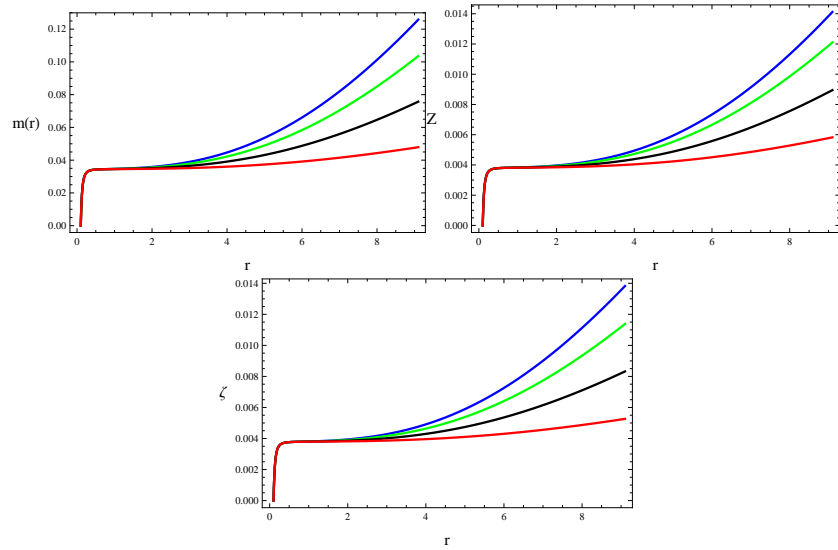


Figure 8: Behavior of mass, redshift and compactness versus  $r$  corresponding to  $\alpha = 0.01$  (Blue),  $0.25$  (Green),  $0.55$  (Black) and  $0.85$  (Red) for solution II.



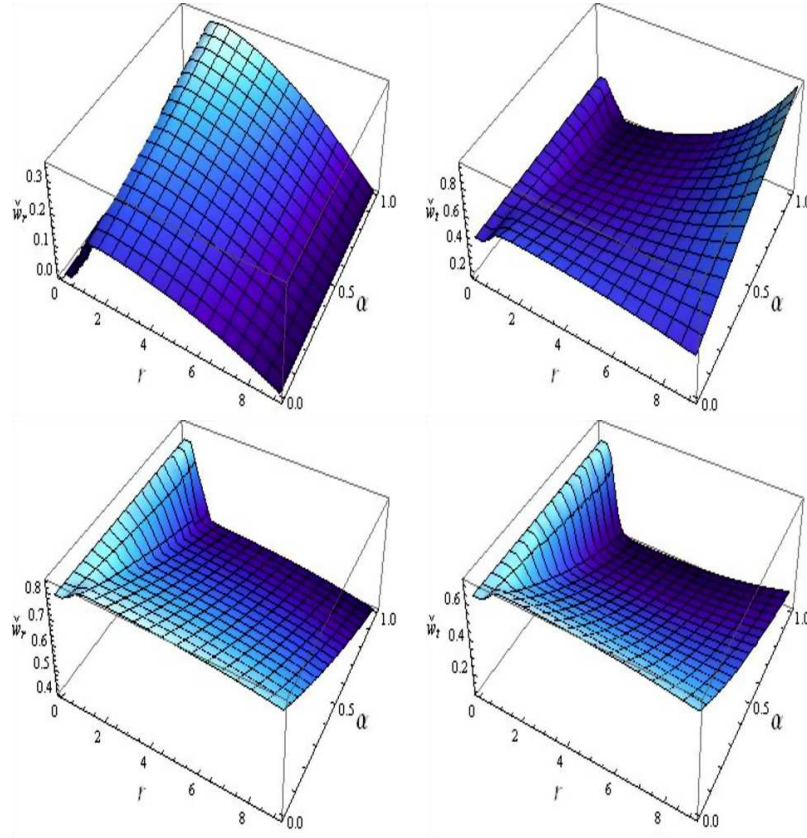


Figure 9: Analysis of components of the equation of state parameters versus  $r$  and  $\alpha$  for solution I and II, respectively.

distribution are evaluated as

$$\check{w}_t = \frac{\check{p}_t}{\check{\rho}}, \quad \check{w}_r = \frac{\check{p}_r}{\check{\rho}}. \quad (58)$$

To examine the nature of matter distribution, the components of the equation of state parameter should be observed from 0 to 1 [47]. Figure 9 indicates that both these parameters, for solutions I and II, satisfy the required limit.

## 6 Conclusions

In the present work, we have developed two anisotropic static spherical solutions for the model  $f(G, T) = \chi G^2 + \psi T$  using EGD scheme. We have induced an extra sector along with the isotropic configuration to generate anisotropy in the system. The field equations have been separated into two independent sets by deforming the radial as well as temporal metric functions, thereby portraying perfect and anisotropic systems. For the isotropic set, we have assumed the Krori-Barua ansatz in which the involved unknown parameters are obtained using matching conditions. The second set (24)-(26) has five unknowns, so we require two more constraints, the equation of state,  $\delta_0^0 = a\delta_1^1 + b\delta_2^2$  and pressure-like or density-like constraint to calculate the anisotropic solutions. Finally, we have examined the viability and stability of the resulting solutions through graphs.

We have utilized energy conditions (54) and three stability criteria to figure out the viability and stability of the resulting anisotropic solutions. The feasibility of both solutions has been confirmed since they meet the limits of energy constraints. Further, both solutions satisfy all three stability criteria (Herrera cracking approach, causality condition and adiabatic index), hence they are stable. The equation of state parameters are also found consistent for both solutions. The mass, redshift and compactness parameters are also inspected for  $\alpha = 0.01, 0.25, 0.55$  and  $0.85$ . The first solution shows little decrement for larger  $\alpha$ , whereas a consequential change has been noticed in the second solution for higher values of  $\alpha$ .

It is interesting to mention here that two anisotropic solutions have been constructed in GR [48] which were found to be unstable in comparison to the present work. In GR, Zubair and Azmat [49] achieved stable configuration only by causality condition, while we have developed solutions that are stable in view of all criteria. Maurya et al. [50] transformed the isotropic source to the anisotropic distribution in  $f(Q)$  gravity (where  $Q$  is non-metricity scalar) and found that stability of the structure is attained only by keeping  $\alpha$  (decoupling parameter) less than 0.18. However, interestingly, it can be seen that our developed models remain stable throughout the whole domain of  $\alpha$ . In  $f(R, T)$  gravity, stable anisotropic decoupled solutions have been generated [51]. Similarly, some viable and stable results have been found in  $f(G)$  gravity [37]. We have also found compatible results here. Finally, we would like to mention that all the results reduce to GR for  $\chi = \psi = 0$  in the model (14).

## Appendix A

The extra curvature terms in  $f(G, T)$  are given as

$$\begin{aligned}
T_0^{0(\text{Cor})} &= \frac{1}{8\pi} \left[ -\frac{1}{2}G^2 + \left( \frac{4e^{-2\vartheta}\varphi''}{r^2} - \frac{4e^{-\vartheta}\varphi''}{r^2} - \frac{2e^{-\vartheta}\varphi'^2}{r^2} + \frac{2e^{-\vartheta}\varphi'\vartheta'}{r^2} \right. \right. \\
&+ \left. \frac{2e^{-2\vartheta}\varphi'^2}{r^2} - \frac{6e^{-2\vartheta}\varphi'\vartheta'}{r^2} \right) G + \left( \frac{12e^{-2\vartheta}\vartheta'}{r^2} - \frac{4e^{-\vartheta}\vartheta'}{r^2} \right) G' \\
&\left. \left( -\frac{8e^{-2\vartheta}}{r^2} + \frac{8e^{-\vartheta}}{r^2} \right) G'' \right], \tag{A1}
\end{aligned}$$

$$\begin{aligned}
T_1^{1(\text{Cor})} &= \frac{1}{8\pi} \left[ \frac{1}{2}G^2 + \left( -\frac{4e^{-2\vartheta}\varphi''}{r^2} + \frac{4e^{-\vartheta}\varphi''}{r^2} + \frac{6e^{-2\vartheta}\varphi'\vartheta'}{r^2} - \frac{2e^{-\vartheta}\varphi'\vartheta'}{r^2} \right. \right. \\
&- \left. \frac{2e^{-2\vartheta}\varphi'^2}{r^2} + \frac{2e^{-\vartheta}\varphi'^2}{r^2} \right) G + \left( \frac{12e^{-2\vartheta}\varphi'}{r^2} - \frac{4e^{-\vartheta}\varphi'}{r^2} \right) G' \Big], \tag{A2}
\end{aligned}$$

$$\begin{aligned}
T_2^{2(\text{Cor})} &= \frac{1}{8\pi} \left[ \frac{1}{2}G^2 + \left( -\frac{4e^{-2\vartheta}\varphi''}{r^2} + \frac{4e^{-\vartheta}\varphi''}{r^2} + \frac{2e^{-\vartheta}\varphi'^2}{r^2} - \frac{2e^{-2\vartheta}\varphi'^2}{r^2} \right. \right. \\
&- \left. \frac{2e^{-\vartheta}\varphi'\vartheta'}{r^2} + \frac{6e^{-2\vartheta}\varphi'\vartheta'}{r^2} \right) G + \left( -\frac{6e^{-2\vartheta}\varphi'\vartheta'}{r} + \frac{4e^{-2\vartheta}\varphi''}{r} \right. \\
&\left. \left. + \frac{2e^{-2\vartheta}\varphi'^2}{r} \right) G' + \frac{4e^{-2\vartheta}\varphi'}{r} G'' \right]. \tag{A3}
\end{aligned}$$

The Gauss-Bonnet term as well as its higher derivatives turn out to be

$$G = \frac{1}{r^2} \left[ 2e^{-2\vartheta} \left( (e^\vartheta - 3) \vartheta' \varphi' - (2\vartheta'' + \varphi'^2) (e^\vartheta - 1) \right) \right], \tag{A4}$$

$$\begin{aligned}
G' &= \frac{-1}{r^3} \left[ 2e^{-2\vartheta} \left( -(\vartheta'' (e^\vartheta - 3) - 2\varphi'' (e^\vartheta - 1)) r\varphi' + r\varphi' (e^\vartheta - 6) \vartheta'^2 \right) \right. \\
&+ \vartheta' \left( r \left( -(e^\vartheta - 2) \right) \varphi'^2 + 2\varphi' r (e^\vartheta - 3) - (3e^\vartheta - 7) r\varphi'' \right) - 2\varphi'^2 (e^\vartheta - 1) \\
&\left. - 2(2\varphi'' - r\varphi^{(3)}) (e^\vartheta - 1) \right], \tag{A5}
\end{aligned}$$

$$G'' = \frac{1}{r^4} \left[ 2e^{-2\vartheta} \left( 6 - 6e^\vartheta + \varphi'^2 (r^2 (e^\vartheta - 2) \vartheta'') - 2 \left( \varphi'' (6(e^\vartheta - 1) - r^2 (2e^\vartheta \right) \right) \right]$$

$$\begin{aligned}
& - 5)\vartheta'' + \varphi''^2 r^2 (e^\vartheta - 1) + r(-4\varphi^{(3)} + r\varphi^{(4)})(e^\vartheta - 1) \Big) + r^2(e^\vartheta - 12) \\
& \times \varphi' \vartheta'^3 + \vartheta' \left( \varphi'(-3r^2(e^\vartheta - 6)\vartheta'' + 4r^2(e^\vartheta - 2)\varphi'' + 6(e^\vartheta - 3)) - 4 \right. \\
& \times r\varphi'^2(e^\vartheta - 2) + r((5e^\vartheta - 11)r\varphi^{(3)} - 4\varphi''(3e^\vartheta - 7)) \Big) - r\vartheta'^2 \left( 4r(e^\vartheta \right. \\
& - 5) \varphi'' - 4(e^\vartheta - 6)\varphi' \Big) + r(e^\vartheta - 4)\varphi'^2 + \varphi' r \left( r((e^\vartheta - 3)\vartheta^{(3)} - 2\varphi^{(3)} \right. \\
& \times (e^\vartheta - 1)) - 4(e^\vartheta - 3)\vartheta'' + 8(e^\vartheta - 1)\varphi'' \Big) \Big]. \tag{A6}
\end{aligned}$$

## Appendix B

The radial component of adiabatic index corresponding to solutions I and II are

$$\begin{aligned}
\check{\Gamma}_r = & \{8\pi(\psi + 4\pi)r^2(2(L + X) - T_0^{0(\text{Cor})}e^{r^2X} - T_1^{1(\text{Cor})}e^{r^2X})(\alpha\psi^2 + 12\pi\alpha\psi \\
& + 32\pi^2\alpha + 4\pi\psi + 2\alpha\psi^2Lr^4X + 24\pi\alpha\psi Lr^4X + 64\pi^2\alpha Lr^4X + 12\pi\psi Lr^4X \\
& + 64\pi^2Lr^4X + 4\pi\psi r^4X^2 + \alpha\psi^2r^2X - \alpha\psi^2e^{r^2X} + 12\pi\alpha\psi r^2X - 12\pi\alpha\psi e^{r^2X} \\
& + 32\pi^2\alpha r^2X - 32\pi^2\alpha e^{r^2X} + 4\pi\psi r^2X - 4\pi\psi e^{r^2X} + 32\pi^2r^2X - 32\pi^2e^{r^2X} \\
& + \pi\psi r^3e^{r^2X}T_0^{0(\text{Cor})'} + \pi(3\psi + 16\pi)r^3e^{r^2X}T_1^{1(\text{Cor})}' + 32\pi^2)\} \{(\alpha\psi^2 + 12\pi\alpha\psi \\
& + 32\pi^2\alpha + 4\pi\psi + 2\alpha\psi^2Lr^2 + 24\pi\alpha\psi Lr^2 + 64\pi^2\alpha Lr^2 + 12\pi\psi Lr^2 + 64\pi^2Lr^2 \\
& - 2\pi\psi r^2T_0^{0(\text{Cor})}e^{r^2X} - 2\pi(3\psi + 16\pi)r^2T_1^{1(\text{Cor})}e^{r^2X} - \alpha\psi^2e^{r^2X} - 12\pi\alpha\psi e^{r^2X} \\
& - 32\pi^2\alpha e^{r^2X} + 4\pi\psi r^2X - 4\pi\psi e^{r^2X} - 32\pi^2e^{r^2X} + 32\pi^2)(-\alpha\psi^2 - 12\pi\alpha\psi \\
& - 32\pi^2\alpha - 4\pi\psi - 2\alpha\psi^2Lr^4X - 24\pi\alpha\psi Lr^4X - 64\pi^2\alpha Lr^4X + 4\pi\psi Lr^4X \\
& + 12\pi\psi r^4X^2 + 64\pi^2r^4X^2 - \alpha\psi^2r^2X + \alpha\psi^2e^{r^2X} - 12\pi\alpha\psi r^2X + 12\pi\alpha\psi e^{r^2X} \\
& - 32\pi^2\alpha r^2X + 32\pi^2\alpha e^{r^2X} - 4\pi\psi r^2X + 4\pi\psi e^{r^2X} - 32\pi^2r^2X + 32\pi^2e^{r^2X} \\
& + \pi(3\psi + 16\pi)r^3e^{r^2X}T_0^{0(\text{Cor})}' + \pi\psi r^3e^{r^2X}T_1^{1(\text{Cor})}' - 32\pi^2)\}^{-1}, \tag{B1}
\end{aligned}$$

$$\begin{aligned}
\check{\Gamma}_r = & \{8\pi(\psi + 4\pi)r^2(2(L + X) - T_0^{0(\text{Cor})}e^{r^2X} - T_1^{1(\text{Cor})}e^{r^2X})(-\alpha\psi^2 - 12\pi\alpha\psi \\
& - 32\pi^2\alpha + 4\pi\psi + 12\pi\psi Lr^4X + 64\pi^2Lr^4X + 2\alpha\psi^2r^4X^2 + 24\pi\alpha\psi r^4X^2 \\
& + 64\pi^2\alpha r^4X^2 + 4\pi\psi r^4X^2 - \alpha\psi^2r^2X + \alpha\psi^2e^{r^2X} + 32\pi^2\alpha e^{r^2X} + 4\pi\psi r^2X
\end{aligned}$$

$$\begin{aligned}
& -12\pi\alpha\psi r^2 X + 12\pi\alpha\psi e^{r^2 X} - 32\pi^2\alpha r^2 X - 4\pi\psi e^{r^2 X} + 32\pi^2 r^2 X - 32\pi^2 e^{r^2 X} \\
& + \pi\psi r^3 e^{r^2 X} T_0^{0(\text{Cor})'} + \pi(3\psi + 16\pi)r^3 e^{r^2 X} T_1^{1(\text{Cor})'} + 32\pi^2) \{ (-\alpha\psi^2 - 12\pi\alpha\psi \\
& - 32\pi^2\alpha + 4\pi\psi + 12\pi\psi Lr^2 + 64\pi^2 Lr^2 - 2\pi\psi r^2 T_0^{0(\text{Cor})} e^{r^2 X} - 2\pi(3\psi + 16\pi)r^2 \\
& \times T_1^{1(\text{Cor})} e^{r^2 X} + 2\alpha\psi^2 r^2 X + \alpha\psi^2 e^{r^2 X} + 24\pi\alpha\psi r^2 X + 12\pi\alpha\psi e^{r^2 X} + 64\pi^2\alpha r^2 X \\
& + 32\pi^2\alpha e^{r^2 X} + 4\pi\psi r^2 X - 4\pi\psi e^{r^2 X} - 32\pi^2 e^{r^2 X} + 32\pi^2) (\alpha\psi^2 + 12\pi\alpha\psi + 32\pi^2\alpha \\
& - 4\pi\psi + 4\pi\psi Lr^4 X - 2\alpha\psi^2 r^4 X^2 - 24\pi\alpha\psi r^4 X^2 - 64\pi^2\alpha r^4 X^2 + 12\pi\psi r^4 X^2 \\
& + 64\pi^2 r^4 X^2 + \alpha\psi^2 r^2 X - \alpha\psi^2 e^{r^2 X} + 12\pi\alpha\psi r^2 X - 12\pi\alpha\psi e^{r^2 X} + 32\pi^2\alpha r^2 X \\
& - 32\pi^2\alpha e^{r^2 X} - 4\pi\psi r^2 X + 4\pi\psi e^{r^2 X} - 32\pi^2 r^2 X + 32\pi^2 e^{r^2 X} + \pi(3\psi + 16\pi)r^3 \\
& \times e^{r^2 X} T_0^{0(\text{Cor})'} + \pi\psi r^3 e^{r^2 X} T_1^{1(\text{Cor})'} - 32\pi^2) \}^{-1}. \tag{B2}
\end{aligned}$$

The expressions of radial velocity in the case of first and second solution are given as

$$\begin{aligned}
\nu_r^2 = & \{ \alpha\psi^2 + 12\pi\alpha\psi + 32\pi^2\alpha + 4\pi\psi + 2\alpha\psi^2 Lr^4 X + 24\pi\alpha\psi Lr^4 X + 64\pi^2\alpha Lr^4 X \\
& + 12\pi\psi Lr^4 X + 64\pi^2 Lr^4 X + 4\pi\psi r^4 X^2 + \alpha\psi^2 r^2 X - \alpha\psi^2 e^{r^2 X} + 12\pi\alpha\psi r^2 X \\
& - 12\pi\alpha\psi e^{r^2 X} + 32\pi^2\alpha r^2 X - 32\pi^2\alpha e^{r^2 X} + 4\pi\psi r^2 X - 4\pi\psi e^{r^2 X} + 32\pi^2 r^2 X \\
& - 32\pi^2 e^{r^2 X} + \pi\psi r^3 e^{r^2 X} T_0^{0(\text{Cor})'} + \pi(3\psi + 16\pi)r^3 e^{r^2 X} T_1^{1(\text{Cor})'} + 32\pi^2 \} \{ -\alpha\psi^2 \\
& - 12\pi\alpha\psi - 32\pi^2\alpha - 4\pi\psi - 2\alpha\psi^2 Lr^4 X - 24\pi\alpha\psi Lr^4 X - 64\pi^2\alpha Lr^4 X \\
& + 4\pi\psi Lr^4 X + 12\pi\psi r^4 X^2 + 64\pi^2 r^4 X^2 - \alpha\psi^2 r^2 X + \alpha\psi^2 e^{r^2 X} - 12\pi\alpha\psi r^2 X \\
& + 12\pi\alpha\psi e^{r^2 X} - 32\pi^2\alpha r^2 X + 32\pi^2\alpha e^{r^2 X} - 4\pi\psi r^2 X + 4\pi\psi e^{r^2 X} - 32\pi^2 r^2 X \\
& + 32\pi^2 e^{r^2 X} + \pi(3\psi + 16\pi)r^3 e^{r^2 X} T_0^{0(\text{Cor})'} + \pi\psi r^3 e^{r^2 X} T_1^{1(\text{Cor})'} - 32\pi^2 \}^{-1}, \tag{B3}
\end{aligned}$$

$$\begin{aligned}
\nu_r^2 = & \{ -\alpha\psi^2 - 12\pi\alpha\psi - 32\pi^2\alpha + 4\pi\psi + 12\pi\psi Lr^4 X + 64\pi^2 Lr^4 X + 2\alpha\psi^2 r^4 X^2 \\
& + 24\pi\alpha\psi r^4 X^2 + 64\pi^2\alpha r^4 X^2 + 4\pi\psi r^4 X^2 - \alpha\psi^2 r^2 X + \alpha\psi^2 e^{r^2 X} - 12\pi\alpha\psi r^2 X \\
& + 12\pi\alpha\psi e^{r^2 X} - 32\pi^2\alpha r^2 X + 32\pi^2\alpha e^{r^2 X} + 4\pi\psi r^2 X - 4\pi\psi e^{r^2 X} + 32\pi^2 r^2 X \\
& - 32\pi^2 e^{r^2 X} + \pi\psi r^3 e^{r^2 X} T_0^{0(\text{Cor})'} + \pi(3\psi + 16\pi)r^3 e^{r^2 X} T_1^{1(\text{Cor})'} + 32\pi^2 \} \{ \alpha\psi^2 \\
& + 12\pi\alpha\psi - 4\pi\psi + 4\pi\psi Lr^4 X - 2\alpha\psi^2 r^4 X^2 - 24\pi\alpha\psi r^4 X^2 - 64\pi^2\alpha r^4 X^2 \\
& + 12\pi\psi r^4 X^2 + 32\pi^2\alpha + 64\pi^2 r^4 X^2 + \alpha\psi^2 r^2 X - \alpha\psi^2 e^{r^2 X} + 12\pi\alpha\psi r^2 X
\end{aligned}$$

$$\begin{aligned}
& - 12\pi\alpha\psi e^{r^2X} + 32\pi^2\alpha r^2X - 32\pi^2\alpha e^{r^2X} - 4\pi\psi r^2X + 4\pi\psi e^{r^2X} - 32\pi^2r^2X \\
& + 32\pi^2e^{r^2X} + \pi(3\psi + 16\pi)r^3e^{r^2X}T_0^{0(\text{Cor})'} + \pi\psi r^3e^{r^2X}T_1^{1(\text{Cor})'} - 32\pi^2\}^{-1}.
\end{aligned}
\tag{B4}$$

## References

- [1] T S Van Albada and R Sancisi *Philos. Trans. Royal Soc. A* **320** 447 (1986); R A Swaters, B F Madore and M Trewhella *Astrophys. J.* **531** L107 (2000)
- [2] J D Barrow, R Maartens and C G Tsagas *Phys. Rep.* **449** 131 (2007); J Neveu, V Ruhlmann-Kleider, P Astier, M Besancon, J Guy, A Moller and E Babichev *Astron. Astrophys.* **600** A40 (2017)
- [3] N Deruella *Nuclear. Phys. B* **327** 253 (1989); N Deruella and L Farina-Busto *Phys. Rev. D* **41** 3696 (1990)
- [4] B Bhawal and S Kar *Phys. Rev. D* **46** 2464 (1992); N Deruella and T Dolezel *Phys. Rev. D* **10** 103502 (2000)
- [5] S Nojiri and S D Odintsov *Phys. Lett. B* **631** 1 (2005)
- [6] S Capozziello, A Stabile, and A Troisi *Class. Quantum Gravit.* **25** 085004 (2008); S Capozziello, E De Filippis, and V Salzano *Mon. Not. R. Astron. Soc.* **394** 947 (2009); S Nojiri and S D Odintsov *Phys. Rep.* **505** 59 (2011).
- [7] O Bertolami, C G Boehmer, T Harko and F S N. Lobo, *Phys. Rev. D* **75** 104016 (2007).
- [8] T Harko, F S N Lobo, S Nojiri, and S D Odintsov *Phys. Rev. D* **84** 024020 (2011).
- [9] M Sharif and A Ikram *Eur. Phys. J. C* **76** 640 (2016)
- [10] M Sharif and A Ikram *Phys. Dark Universe* **17** 1 (2017)
- [11] G Mustafa, X Tie-Cheng and M F Shamir *Ann. Phys.* **413** 168059 (2020)

- [12] M Sharif and K Hassan *Pramana* **96** 50 (2022); *Eur. Phys. J. Plus* **137** 1380 (2022); *Mod. Phys. Lett. A* **37** 2250027 (2022); *Eur. Phys. J. Plus* **138** 787 (2023); *Chin. J. Phys* **77** 1479 (2022); *Chin. J. Phys* **84** 152 (2023)
- [13] M Ruderman *Annu. Rev. Astron. Astrophys.* **10** 427 (1972)
- [14] A I Sokolov *J. Exp. Theor. Phys.* **49** 1137 (1980)
- [15] R Kippenhahn, A Weigert and A Weiss *Stellar Structure and Evolution* (Berlin: Springer-verlag) (1990)
- [16] L Herrera and N O Santos *Phys. Rep.* **286** 53 (1997)
- [17] T Harko and M K Mak *Ann. Phys.* **11** 3 (2002)
- [18] K Dev and M Gleiser *Gen. Relativ. Gravit.* **34** 1793 (2002)
- [19] B C Paul and R Deb *Astrophys. Space Sci.* **354** 421 (2014)
- [20] J D V Arbanil and M Malheiro *J. Cosmol. Astropart. Phys.* **11** 012 (2016)
- [21] A Errehymy, Y Khedif and M Daoud *Eur. Phys. J. C* **81** 266 (2021)
- [22] S K Maurya, S D Maharaj, J Kumar and A K Prasad *Gen. Relativ. Gravit.* **51** 86 (2019)
- [23] G Abbas, D Momeni, M Aamir Ali, R Myrzakulov and S Qaisar *Astrophys. Space Sci.* **357** 158 (2015); M Ilyas *Eur. Phys. J. C* **78** 757 (2018)
- [24] M F Shamir and S Zia *Eur. Phys. J. C* **77** 448 (2017)
- [25] J Ovalle *Phys. Rev. D* **95** 104019 (2017)
- [26] J Ovalle, R Casadio, R da Rocha, A Sotomayor and Z Stuchlik *Eur. Phys. J. C* **78** 960 (2018)
- [27] L Gabbanelli, A Rincon and C Rubio *Eur. Phys. J. C* **78** 370 (2018)
- [28] M Estrada and F Tello-Ortiz *Eur. Phys. J. Plus* **133** 453 (2018)

- [29] K N Singh, S K Maurya, M K Jasim and F Rahaman *Eur. Phys. J. C* **79** 851 (2019)
- [30] S Hensh and Z Stuchlik *Eur. Phys. J. C* **79** 834 (2019)
- [31] M Sharif and S Saba *Chin. J. Phys.* **59** 481 (2019); *Chin. J. Phys.* **63** 348 (2020)
- [32] M Sharif and A Waseem *Chin. J. Phys.* **60** 426 (2019); *Ann. Phys.* **405** 14 (2019); M Sharif and A Majid *Chin. J. Phys.* **68** 406 (2020); *Phys. Dark Universe* **30** 100610 (2020); S K Maurya, A Errehymy, K N Singh, F Tello-Ortiz and M Daoud *Phys. Dark Universe* **30** 100640 (2020); S K Maurya, F Tello-Ortiz and S Ray *Phys. Dark Universe* **31** 100753 (2021); M Sharif and T Naseer *Chin. J. Phys.* **73** 179 (2021); T Naseer and M Sharif *Universe* **8** 62 (2022); M Sharif and T Naseer *Eur. Phys. J. Plus* **137** 1304 (2022)
- [33] M Sharif and K Hassan *Eur. Phys. J. Plus* **137** 997 (2022); *Int. J. Geom. Methods Mod. Phys.* **19** 2250150 (2022); *Int. J. Geom. Methods Mod. Phys* **20** 2350100 (2023); K Hassan and M Sharif *Universe* **9** 165 (2023)
- [34] J Ovalle *Phys. Lett. B* **788** 213 (2019)
- [35] E Contreras and P Bargueño *Class. Quantum Gravit.* **36** 215009 (2019)
- [36] M Sharif and Q Ama-Tul-Mughani *Ann. Phys.* **415** 168122 (2020); *Chin. J. Phys.* **65** 207 (2020)
- [37] M Sharif and S Saba *Int. J. Mod. Phys. D* **29** 2050041 (2020)
- [38] J Schutz and F Bernard *Phys. Rev. D* **2** 2762 (1970)
- [39] M F Shamir and M Ahmad *Eur. Phys. J. C* **77** 674 (2017); M Sharif and A Naeem *Int. J. Mod. Phys. A* **35** 2050121 (2020)
- [40] K D Krori and J Barua *J. Phys. A Math. Gen.* **8** 508 (1975)
- [41] T Guver, P Wroblewski, L Camarota and F Özel *Astrophys. J.* **719** 1807 (2010)



- [42] H Abreu, H Hernandez and L A Nunez *Class. Quantum Gravit.* **24** 4631 (2007)
- [43] L Herrera *Phys. Lett. A* **165** 206 (1992)
- [44] H Heintzmann and W Hillebrandt *Astron. Astrophys.* **38** 51 (1975)
- [45] H A Buchdahl *Phys. Rev.* **116** 1027 (1959)
- [46] B V Ivanov *Phys. Rev. D* **65** 104011 (2002)
- [47] G Mustafa, M F Shamir, M Ahmad and A Ashraf *Chin. J. Phys.* **67** 576 (2020)
- [48] M Sharif and S Sadiq *Eur. Phys. J. C* **78** 410 (2018)
- [49] M Zubair and H Azmat *Ann. Phys.* **420** 168248 (2020)
- [50] S K Maurya, A Errehymy, M K Jasim, M Daoud, N Al-Harbi and A H Abdel-Aty *Eur. Phys. J. C* **83** 317 (2023)
- [51] Q Muneer, M Zubair and M Rahseed *Phys. Scr.* **96** 125015 (2021); M Sharif and F Furqan *Indian J. Phys.* **96** 3375 (2022)